

10-14 July 2016, Vienna, Austria

Investigation of Desiccants and CO₂ Sorbents for Advanced Exploration Systems 2015-2016

James C. Knox¹, David W. Watson², Charles D. Wingard³, Phillip W. West⁴,
NASA/Marshall Space Flight Center, Huntsville, Alabama, 35812

Gregory E. Cmarik⁵, and Lee A. Miller⁶
Jacobs ESSSA Group, Huntsville, Alabama, 35812

Advanced Exploration Systems are integral to crewed missions beyond low earth orbit and beyond the moon. The long-term goal is to reach Mars and return to Earth, but current air revitalization systems are not capable of extended operation within the mass, power, and volume requirements of such a mission. Two primary points are the mechanical stability of sorbent pellets and recovery of sorbent productivity after moisture exposure in the event of a leak. In this paper, we discuss the present efforts towards screening and characterizing commercially-available sorbents for extended operation in desiccant and CO₂ removal beds.

Nomenclature

4BMS	=	Four-Bed Molecular Sieve
ARREM	=	Atmosphere Resource, Recovery and Environmental Monitoring
AES	=	Advanced Exploration Systems
CDRA	=	Carbon Dioxide Removal Assembly
HST	=	Hydrothermal Stability Test
ISS	=	International Space Station
LSS	=	Life Support Systems
NASA	=	National Aeronautics and Space Administration
BET	=	Brunauer, Emmett, and Teller
mmHg	=	millimeter of mercury (Torr)
slpm	=	standard liters per minute (STP = 0°C, 760 mmHg)
LiLSX	=	Lithium, Low-Silica X-type Zeolite

I. Introduction

THE Atmosphere Revitalization Recovery and Environmental Monitoring (ARREM) project is a segment of the Advanced Exploration Systems (AES) program. The stated purpose of the AES program is “pioneering innovative approaches and public-private partnerships to rapidly develop prototype systems, advance key capabilities, and validate operational concepts for future human missions beyond Earth orbit.”¹ This program is being applied to long-term crewed missions, a task which places extreme demands on individual systems. A CO₂ removal system which utilizes beds of desiccants and molecular sieves is known as four-bed molecular sieve (4BMS). This work focuses on the properties of these materials and the results of this work will be applied to future 4BMS systems for exploration missions and to improve the system in use onboard the ISS.

In order to enable a 4-person crew to successfully reach and return from Mars or other deep space location, systems for removal of metabolic carbon dioxide must reliably operate for several years while minimizing power, mass, and volume requirements. This minimization can be achieved through system redesign and/or changes to the separation

¹ Aerospace Engineer, Environmental Control and Life Support Development Branch/ES62

² Mechanical Engineer, Environmental Control and Life Support Development Branch/ES62

³ Mechanical Engineer, Materials Testing/EM10

⁴ Mechanical Engineer, Environmental Control and Life Support Development Branch/ES62

⁵ Chemical Engineer, Environmental Control and Life Support Development Branch/ES62

⁶ Senior Engineer, Environmental Control and Life Support Development Branch/ES62

material(s). A screening process is required to make the best material selection for a future closed-loop carbon dioxide removal system. The results of this screening process will provide the information necessary to guide system design as well as provide risk assessment and means for risk mitigation.

On board the ISS, the system tasked with removal of the metabolic carbon dioxide is a specialized 4BMS known as CDRA. A schematic of a 4BMS system is shown in Figure 1. The materials used in the desiccant beds are layers of silica gels and 13X zeolite which reduce inlet dew points to -90°C or lower while CO_2 removal beds contain pelletized 5A zeolites. The present CDRA system maintains a cabin CO_2 concentration of 3 torr on the ISS but new requirements seek to reduce this to 2 torr to improve crew health and mission effectiveness. This reduced concentration leads to increased power requirements and reduced operating lifespan of CDRA. Also, the current CO_2 sorbent, ASRT, can no longer be produced which necessitates the selection of an alternative CO_2 sorbent for CDRA. The search for robust materials with improved properties for the long-term, cyclic operation of CDRA and of an exploration 4BMS is the focus of this work.

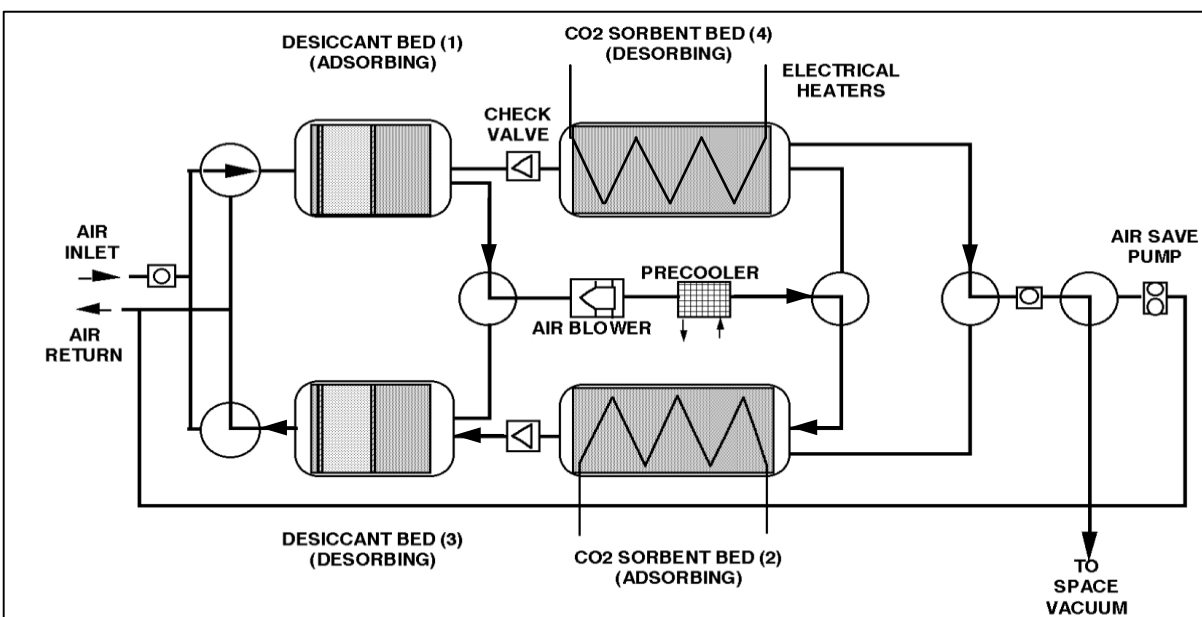


Figure 1. Schematic of a 4BMS depicting one half-cycle of operation. Humid cabin air flows through adsorbing desiccant bed (1) and then through a blower and precooler. This cool, dry air passes through a pelletized zeolite sorbent bed (2) where CO_2 is adsorbed and then through desorbing desiccant bed (3). Sorbent bed (2) retains heat from regeneration in the previous half-cycle and this residual heat provides a hot purge to desorb water from the adjacent desiccant bed (3). During this half-cycle, the alternate CO_2 sorbent bed (4) is heated and evacuated to regenerate the sorbent material.

The desiccant beds are composed of multiple layers: guard, bulk removal, and residual removal. The guard layer is composed of a robust material at the front of the bed which captures any entrained liquid water droplets (misting), but these materials have lower capacity. Liquid water contact would cause the high capacity silica gel in the bulk removal layer to fracture on contact. The residual removal layer is a zeolite with high water affinity and fast kinetics in order to adsorb all measurable traces of water. The CO_2 removal beds in the current CDRA configuration are uniform beds of 5A zeolite with an embedded heating element with a design operating temperature of 400°F (204°C).

The characterization and screening of candidate materials is focused on commercially available sorbents but also includes custom sorbents when available. Table 1 provides a list of materials included in this screening study and general characteristics. Initial screening with sample quantities of each material involves single-pellet crush testing, pure component CO_2 adsorption at multiple temperatures, and working capacity testing after humidity conditioning. Further characterization is conducted when more extensive quantities are available which involves bulk crush and attrition testing as well as packed bed breakthrough testing. While a general overview of structural properties for selection is given in this work, detailed study of the structural properties is given in the work submitted for publication by Weston.² A simplification of the sorbent performance factors table from the work by Knox³ is shown in Table 2 and provides the properties obtained in these tests along with how they are to be utilized.

Table 1. Materials Included in the Sorbent Screening Study

Material Type	Sorbent Name	Use/Potential Use	Form Factor	Pore size	Notes
Silica Gel	Grace Grade 40	Bulk Desiccant	Granular	Microporous	-
Silica Gel	Grace SG B125	Bulk Desiccant	Beads	Microporous	-
Silica Gel	BASF Sorbead R	Bulk Desiccant	Beads	Microporous	-
Silica Gel	BASF Sorbead H	Bulk Desiccant	Beads	Microporous	-
Alumino-Silica Gel	BASF Sorbead WS	Guard Layer	Beads	Microporous	Misting Stable
Activated Alumina	BASF F200	Bulk Desiccant	Beads	Mesoporous	Misting Stable
Molecular Sieve	Grace MS 564	Residual Desiccant	Beads	3Å	KA Zeolite
Molecular Sieve	Grace MS 514	CO ₂ sorbent, Residual Desiccant	Beads	4Å	NaA Zeolite
Molecular Sieve	Grace MS 522	CO ₂ sorbent, Residual Desiccant	Beads	5Å	CaA Zeolite
Molecular Sieve	Grace MS 544	CO ₂ sorbent, Residual Desiccant	Beads	10Å	NaX Zeolite
Molecular Sieve	BASF 5A	CO ₂ sorbent, Residual Desiccant	Beads	5Å	CaA Zeolite
Molecular Sieve	BASF 13X	CO ₂ sorbent, Residual Desiccant	Beads	10Å	NaX Zeolite
Molecular Sieve	BASF 5A BF	CO ₂ sorbent	Beads	5Å	CaA Zeolite, Binder-free
Molecular Sieve	BASF 13X BF	CO ₂ sorbent	Beads	10Å	NaX Zeolite, Binder-free
Molecular Sieve	UOP APGIII	CO ₂ sorbent	Beads	10Å	NaX Zeolite
Molecular Sieve	UOP VSA-10	CO ₂ sorbent	Beads	10Å	LiLSX Zeolite
Molecular Sieve	UOP ASRT	CO ₂ sorbent	Pellets	5Å	CaA Zeolite, used in CDRA
Molecular Sieve	UOP RK-38	CO ₂ sorbent	Beads	5Å	CaA Zeolite, used in CDRA
Molecular Sieve	UOP Polymer-IEX	CO ₂ sorbent	Pellets	10Å	LiLSX Zeolite, Polymer-Binder
Molecular Sieve	Zeochem Z05-01	CO ₂ sorbent	Beads	5Å	CaA Zeolite
Molecular Sieve	Zeochem Z10-02	CO ₂ sorbent	Beads	10Å	NaX Zeolite

Table 2. Sorbent Screening Performance Factors

Intrinsic Performance Factors	Screening Criteria	Simulation Input	Extrinsic/Pellet Performance Factors	Screening Criteria	Simulation Input
Single Gas Equilibrium Capacity	✓	✓	Single Pellet Crush Strength	✓	
Heat of Adsorption	✓	✓	Pellet Friability	✓	
Adsorption Kinetics	✓	✓	Bulk Crush Strength	✓	
Moisture Sensitivity	✓		Thermal Stability	✓	
			Packing Density/ Pressure Drop	✓	✓

The structural tests utilized in this and previous studies originate from industry standards and have been augmented to more closely match observed and theorized conditions in CDRA.³ Breakdown of sorbent pellets is a known phenomenon in industry where replacement is merely undesirable but poses a unique challenge for a long-term mission where replacement may be impossible. Theorized causes include thermal cycling, abrasion due to vibrations and localized fluidization, the forces experienced during compaction and flight, and exposure to trace levels of humidity. These pellet degradation mechanisms are simulated with the single pellet crush, bulk crush, and attrition tests⁴ as well as cyclic hydrothermal testing.⁵

The purpose of this sorbent screening study is to gather relevant information for ranking sorbents, provide data for future 4BMS design and optimization, and determine the feasibility of drop-in replacement sorbents for CDRA. The adsorption and breakthrough tests enable simulation of CO₂ removal performance. The adsorption tests with humidity conditioning are used for risk assessment regarding drop-in use in CDRA as well as providing design criteria for future 4BMS systems. The humidity conditioned tests were developed in response to water entering systems downstream of CDRA which indicated water in the CO₂ sorbent bed(s). The structural tests allow ranking of pellet performance and are related to various possible sources of pellet degradation in a 4BMS.

II. Experimental (test description, ASTM methods, references)

A. Structural Test Procedures

The structural test procedures are based on their respective ASTM methods. For the data reported in this paper, dry single pellet crush tests follow ASTM D4179-03 Standard Test Method for Single Pellet Crush Strength of Formed Catalysts and Catalyst Carriers. Details on methods for determining the pellet crush properties listed in this work can be found in the works by Knox³ and by Watson.⁴ Additionally, the work by Watson details bulk crush and attrition testing as well as the augmented methods developed to test structural properties for materials under controlled humidity conditions. The data obtained in the single pellet crush test include the mean and variance among crush strengths for the 50 pellet test lots. Also, during the crush of each pellet, dusting can occur which is the release of fine particles prior to the ultimate crush strength. The fraction of pellets in each test lot which dust and the mean force applied to initiate dusting are also recorded.

B. Adsorption Test Procedures

The adsorption test procedures were developed specifically for the test stands built at the NASA facility. Breakthrough test procedure ES62-TCP-SORB-14-006 details the steps required to utilize the Cylindrical Breakthrough Test (CBT) stand. The measurements and controls available to the CBT stand enable precise control and data acquisition. Measurement of bed pressure, differential pressure, temperature profile at the centerline and at the container exterior, and sampling of gas concentrations at the inlet and outlet of the bed enable this high fidelity. The results from this test can be used further to validate computer simulations and thus model dynamic adsorption behavior.

The Humidity Conditioning Stand (HCS) is designed to provide a constant supply of low dew point N₂ to six ports in parallel. This system has high accuracy dew point sensors and achieves dew point control by mixing dry N₂ with a

small amount of humidified gas controlled via a feedback control loop. Due to the extremely low quantity of water vapor supplied to each port, breakthrough experiments can be conducted as the breakthrough time is much longer than other transient effects. Although the lack of control prevents precise fitting of a model to extract dynamic behavior, equilibrium capacity and relative adsorption kinetics can be obtained. For each test, samples were dried at 350°C in dry N₂ and transferred to a glove box where 20.0g was placed into each test cell. Repeated tests were conducted by reactivating the test cell and sample in an oven at 350°C, cooling in the glove box, and replication of the test.

The Hydrothermal Stability Test (HST) stand⁵ is designed to expose a small-scale sorbent bed to temperature cycles and a N₂ stream with a controllable dew point. The HST was designed in response to evidence of water entering the CO₂ sorbent beds on station. This instrument can also test CO₂ breakthrough of a bed both before and after exposure to moisture and subsequent regeneration at 204°C. The breakthrough curves obtained from this instrument are integrated to obtain CO₂ capacity at 50% breakthrough (bulk separation) and at saturation. In order to obtain breakthrough curves with fully activated samples, the sorbent was activated at 350°C in an oven then packed in the HST beds in a glove box prior to breakthrough testing. Humidity conditioning and subsequent regeneration in dry N₂ at 204°C was achieved *in situ* using the available test stand components.

The working capacity tests were conducted on a SETARAM Sensys Evo thermogravimetric analysis (TGA) instrument. The available controls allowed for a study of the working capacity of CO₂ at constant ambient pressure after varying sample activation time and temperature. Each sample of roughly 10 pellets was left exposed to ambient lab air for several days to allow for adsorption of a high level of water vapor prior to testing. The samples were then activated at incrementally higher temperatures for 4 hours. Each of these heating cycles was followed by an adsorption cycle at 25°C and 0.5% CO₂. Another sample was prepared and then cyclically tested under a series of simulated CDRA heating cycles then further activated at moderately elevated temperatures for 10 hours. Each of these heating cycles was followed by an adsorption cycle at 25°C and 0.5% CO₂ as well. These tests constitute a risk assessment via comparison of the working capacity of each material after a simulated off-nominal event. The results can guide future 4BMS designs and improve the procedures for CDRA.

III. Results and Discussion

A. Desiccant selection

The desiccant beds in a 4BMS system consist of three layers: guard, bulk water removal, and residual water removal. The guard layer is a thin layer of material with the purpose of withstanding liquid water contact and protecting the bulk desiccant. The bulk water removal layer consists of a silica gel and this bed layer is sized to remove nearly all incoming water vapor. The residual water removal layer consists of a pelletized zeolite, such as a 13X zeolite, which can reduce outlet dew points below -90°C. The current materials in use for these three layers are BASF Sorbead WS, Grace Sylobead SG B125, and Grace Sylobead MS 544 13X, respectively.

The structural properties of various materials under consideration for the bulk water removal layer are shown in Figure 2. The materials are grouped by their shape and whether the material is stable to contact with liquid water droplets, referred to as ‘misting’. For many silica gels, misting induces particle fracture with a select example shown in the photos reproduced in Figure 3. Particle fracture leads to increased bed pressure drop and increased local voids which allow for further particle movement and attrition.

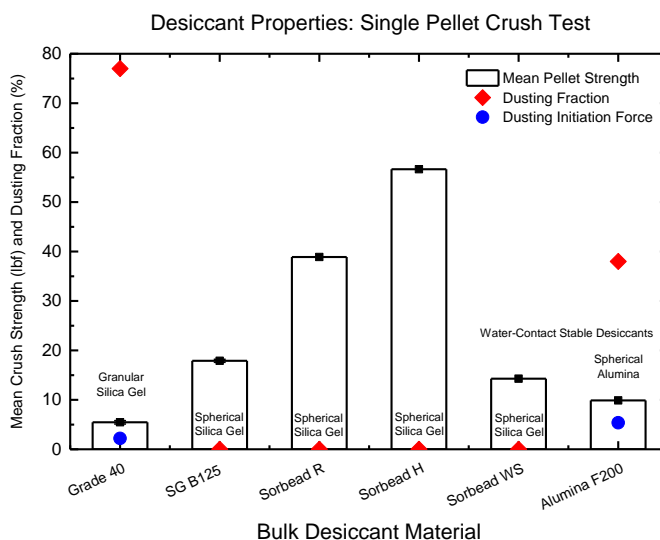


Figure 2. Single pellet mean crush strength, mean crush strength span (error bar), dusting fraction, and dusting initiation force results for six desiccants. Crush strength span is the range between means measured among 3 tests. Dusting fraction is the ratio of pellets which fractured in a manner producing dust prior to completion. Dusting onset strength is the average crush strength where dusting was observed to begin to occur and is set to zero if no dusting is observed.

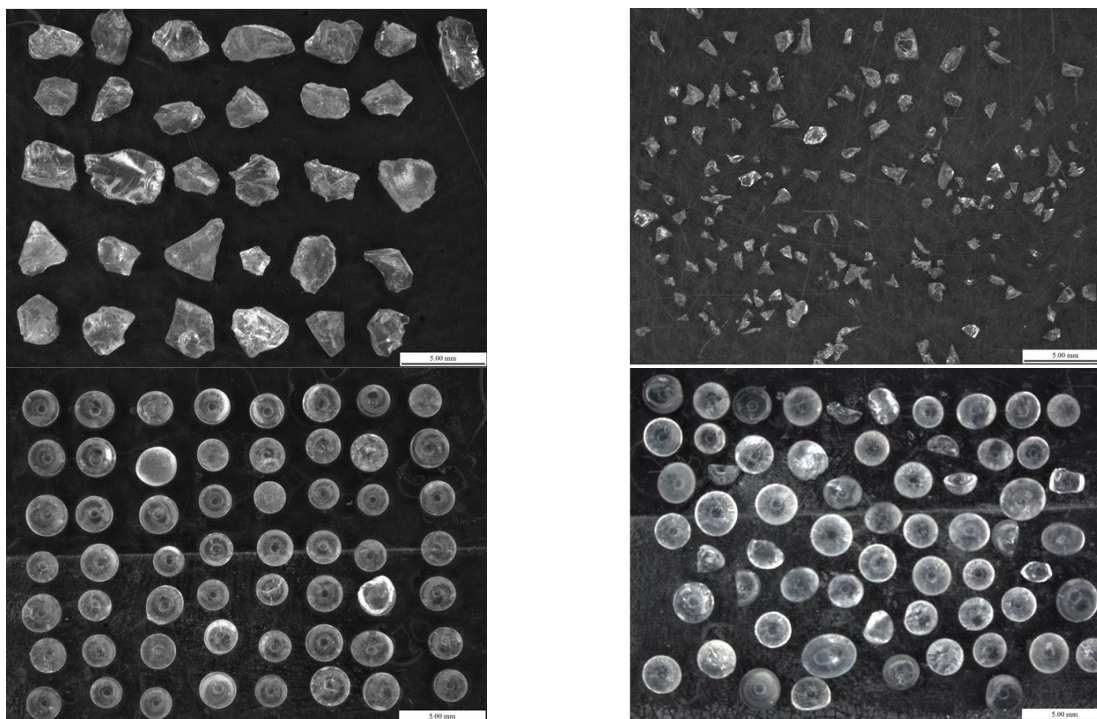


Figure 3. Fracturing of Grace Grade 40 (top) and Grace SG B125 (bottom) silica gel particles before (left) and after (right) contact with liquid water in a misting test. Fracturing on contact with liquid water is a phenomenon common to high capacity silica gels.

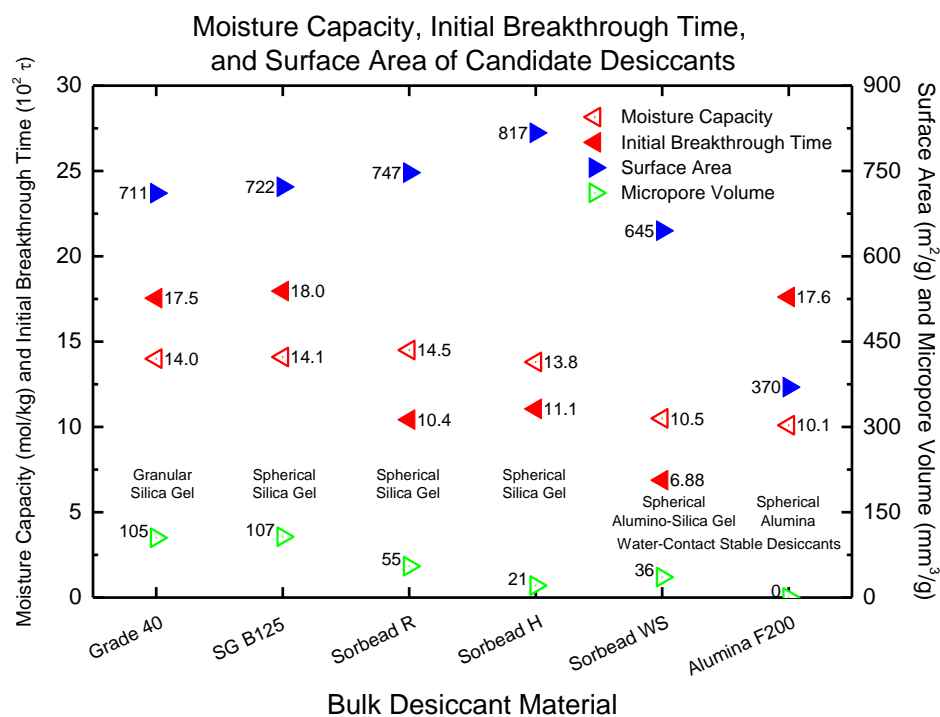


Figure 4. Dynamic moisture capacity ($mol\ H_2O/kg$ sorbent), initial breakthrough time ($10^2 \tau$), BET surface area (m^2/g), and micropore volume (mm^3/g) for the six desiccants studied. Initial breakthrough time is when 5% of inlet moisture content is observed at the outlet of the bed. The bed residence time (τ) was 0.543 sec.

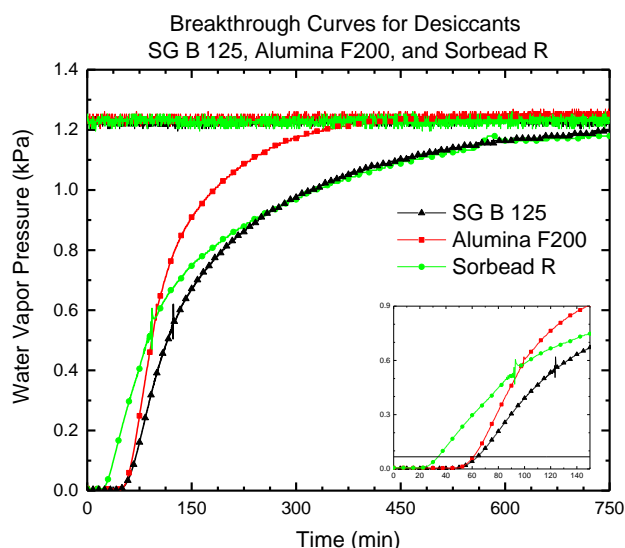


Figure 5. Breakthrough plots for Sorbead R, SG B125, and Alumina F200 at 25°C when challenged with an inlet dew point of 10°C. The water vapor concentration used to determine initial breakthrough time is marked on the inset with a horizontal line.

Sorbead H at 0.55 cm³/g. Due to these similarities, micropore volume was considered instead and roughly correlated with initial breakthrough time. Breakthrough time was considered to distinguish between the materials as it can also be used as a rough estimate for bed layer sizing. This value was determined at the point in time where 5% of the feed concentration of water vapor is measured exiting the bed and is reported in bed residence time (τ). Micropore volume was found to roughly correlate with breakthrough time except for Sorbead H and Alumina F200 where breakthrough time exceeded the otherwise observed trend. An overlay of breakthrough curves for Sorbead R, SG B125, and Alumina F200 is provided in Figure 5 to illustrate the difference in performance of a packed bed of each material.

SG B125 possesses a high water capacity and the longest initial breakthrough time which is indicative of fast mass transfer rates. Grade 40 shows equal capacity to SG B125 but has a slightly reduced initial breakthrough time and broader mass transfer zone. Sorbead R and H show high capacity but shorter initial breakthrough times than SG B125. Sorbead WS has moderate performance characteristics and short initial breakthrough times. Alumina F200 shows an initial breakthrough time nearly as long as SG B125 despite having a significantly lower maximum water capacity.

When all of these properties are considered, the strongest candidates are Sorbead WS for the guard layer material and SG B125 for the bulk desiccant layer. Extensive analysis would be necessary to differentiate the bulk desiccants further and would involve large-scale tests in cyclic

The single pellet crush strength for Sorbead R, Sorbead H, Sorbead WS, and Sylobead SG B125 is very high and well above the strongest zeolite pellets. Only Grade 40 and SG B125 have been tested multiple times for single pellet crush and the variance among mean crush strengths cannot be discerned from the symbol. This high pellet crush strength is more than sufficient to maintain pellet integrity during assembly and operation as evidenced by past disassembly of flight beds. Additionally these four materials show no dusting during a crush test. The granular silica gel and alumina show significant dusting and have a lower crush strength, on the order of many of the zeolite pellets that have been tested. Sorbead WS and Alumina F200 are observed to be misting stable.

The moisture breakthrough characteristics obtained with the Cylindrical Breakthrough Test (CBT) stand and the pore properties obtained with a Micromeritics TriStar for the six materials is shown in Figure 4. The maximum water capacity and surface area roughly correlate throughout the six desiccants. The total pore volumes for each material were found to be equivalent at 0.44 cm³/g except for

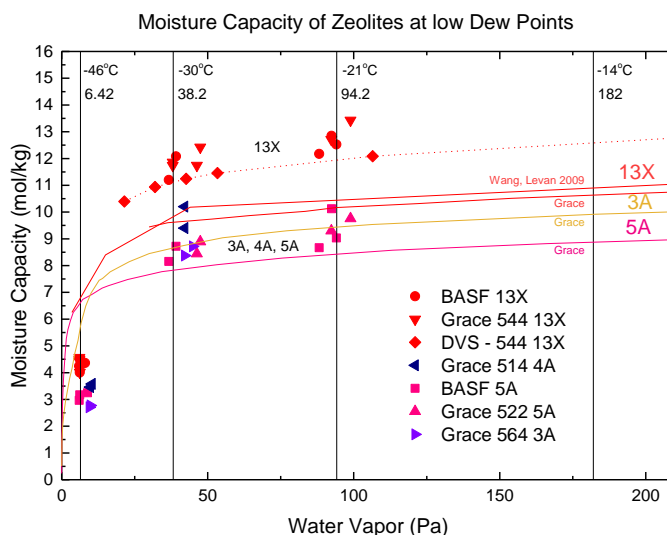


Figure 6. Equilibrium capacity of six candidate residual desiccants measured with the Humidity Conditioning Stand. Tests were conducted at ambient air temperature which averaged 22°C with daily fluctuations. For reference, a partial isotherm obtained with a DVS Vacuum at Ames Research Center, and isotherm from the work by Wang⁶, and a series of isotherms extracted from plots in literature published by Grace all obtained at 25°C are overlaid.

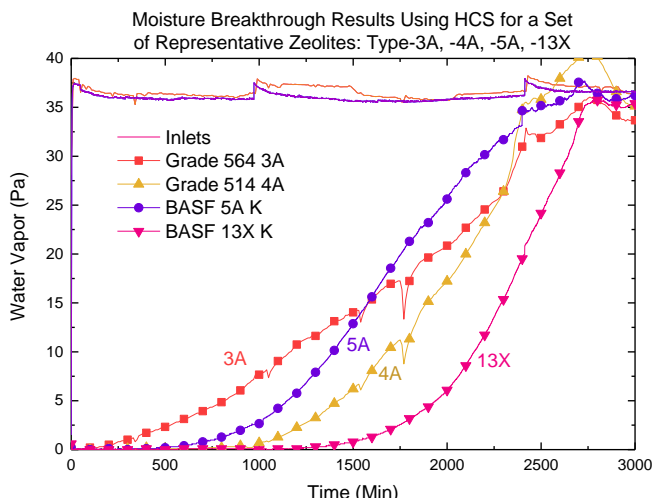


Figure 7. Select breakthrough curves obtained using the Humidity Conditioning Stand for each class of zeolite tested as a residual desiccant.

building operations. Three dew points were selected for these tests, -46°C , -30°C , and -21°C , which were selected to enable comparison with reference data points.

The results of breakthrough capacity of water vapor are shown in Figure 6. In addition, several reference values from manufacturer literature and an isotherm obtained with a DVS Vacuum instrument were overlaid on the plot. The results indicate that 13X zeolites in general adsorb more moisture at all measured dew points in this test followed by the 4A, 5A, and 3A zeolites, respectively.

Four representative breakthrough curves obtained with this test stand at -30°C dew point are shown in Figure 7. The type-13X zeolite has the most ideal breakthrough curve and maintains a dew point below detectable limits for the longest time. The type-A zeolites each show earlier breakthrough and slower adsorption, with the slow kinetics of the type-3A zeolite showing very rapid trace breakthrough. This follows the trend where density of counterions and pore accessibility dictates the performance of these residual desiccants. These results do not provide insight into the performance in cyclic operations due to the lack of heated, counter-current desorption.

From these results, the best selection for the CDRA residual desiccant layer remains a type-13X zeolite. Although no data suggest the 13X currently in use in CDRA should be replaced, there exist system-level considerations which may enable an alternative residual desiccant selection in a future 4BMS system. When dry, 13X zeolite will also adsorb significant amounts of CO_2 and lower the overall system efficiency due to this parasitic capture, whereas a 3A zeolite would not adsorb any CO_2 . Therefore, further tests will be needed to determine if 3A zeolite can provide sufficient desiccation for a future 4BMS system.

B. CO_2 sorbent selection

The CO_2 sorbent beds in a 4BMS system are uniform packed beds of pelletized molecular sieves. The current material in the CO_2 sorbent beds on the ISS is ASRT, a custom sorbent from UOP for CDRA which can no longer be produced, necessitating a selection for CDRA. Additionally, the current target for cabin air CO_2 partial pressure is 2 torr for the ISS and future exploration missions, necessitating high CO_2 removal capacity. In order to accommodate future goals and to improve the power, weight, and volume of a 4BMS system, sorbents which can remove more CO_2 than 5A zeolites are being studied. Type-5A zeolites continue to be studied as they possess favorable regeneration properties for fault recovery from moisture exposure. Type-13X zeolites and ion-exchanged X-type zeolites are being studied as replacement materials due to their high affinity for CO_2 at low partial pressures and rapid adsorption kinetics. Increased CO_2 removal at lower partial pressures is an enabling property for future systems design.

The results of single pellet crush testing of the CO_2 sorbents are shown in Figure 8. The materials are grouped by the type of zeolite contained in the pellets and each material is in the form of spherical beads except ASRT and polymer-bound IEX. Most of these materials have only been tested for single pellet crush strength at dry and humidified conditions due to material quantity limitations.

The mean pellet crush strength in dry conditions shows all but three of the tested materials are weaker than ASRT, with BASF 13X, BASF 13X BF, and Grace Grade 544 13X showing statistically equivalent mean crush strengths.

operation. Therefore, the first two desiccant bed layers remain as they are at present for CDRA and for the initial iterations of a future 4BMS. Alumina may be further studied in cyclic operation to understand whether it outperforms silica gel in this application and if it is sufficiently robust for extended use.

A selection for the residual desiccant (zeolite) layer involves many of the same steps as those taken for bulk desiccant selection. The time scales required to test these materials at low dew points which could best represent the conditions found in the residual desiccant layer necessitated higher sample bandwidth than available with the CBT. An existing test stand with capacity for 6 parallel tests is known as the Humidity Conditioning Stand (HCS). The HCS was selected instead to conduct these trace water vapor breakthrough tests. Dew point control in the HCS is nearly constant except for brief excursions coinciding with the daily cycle of

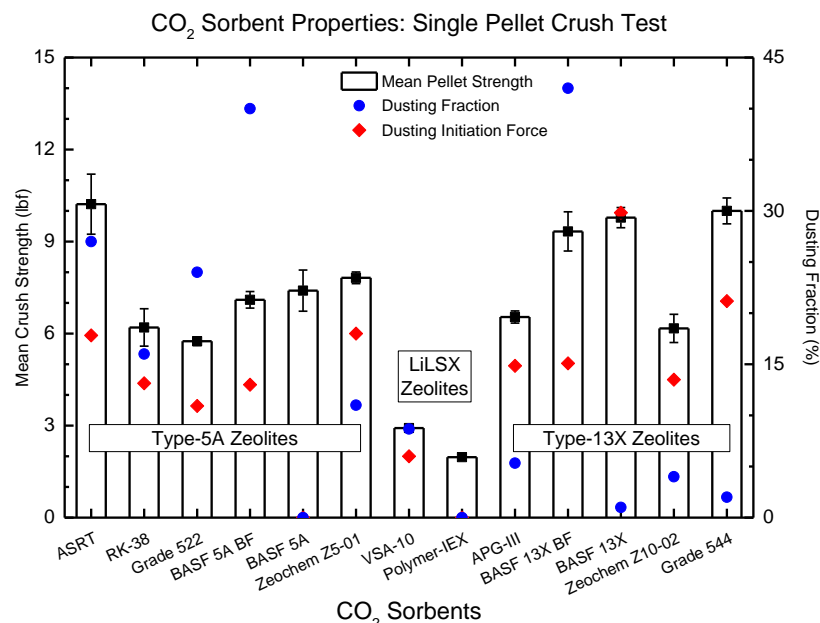


Figure 8. Single pellet mean crush strength, mean crush strength span (error bar), dusting fraction, and dusting initiation force results for 13 CO₂ sorbents.

the worst candidates and is not sufficient to make a further selection. Additionally, the pellet-to-pellet variation is quite large (not shown) for all of these materials due to the brittle nature of clay-bound pellets which further complicates performance predictions. Further structural studies of these materials are provided in the work submitted for publication by Watson.²

The remaining materials are compared on the basis of CO₂ capacity at the partial pressure of past (4 torr) and future (2 torr) space station cabin air CO₂ concentrations. The primary impetus of the reduced cabin concentration is the increasing body of evidence showing the negative effects of CO₂ on health and performance in physical and mental activities.^{7,8} As the target partial pressure of CO₂ drops, the productivity difference between ASRT and some of the candidate materials becomes more pronounced. Figure 9 shows the capacity of zeolites tested to date at 2 torr and 4 torr CO₂ and 25°C.

The materials are grouped by the type of zeolite in the pellets. ASRT can be considered the baseline for required CO₂ capacity and has the highest capacity among type-5A zeolites, with alternatives RK-38 and Grade 522 showing nearly equal capacity. All of the 13X materials exceed ASRT, with APGIII showing the best capacity among those materials, although the zeolite chemistry within this material is not explicitly known. The clay-bound LiLSX zeolite shows exceptional performance while the polymer-bound LiLSX material performs similar to the 13X materials due to a lower density of LiLSX crystals in the pellets.

Although these materials can be ranked with the results from pure component isotherms, the weight-normalized CO₂ capacity can be misleading when directly extrapolated to predict packed bed performance. Most clay-bound zeolites of similar size show similar packing density, but

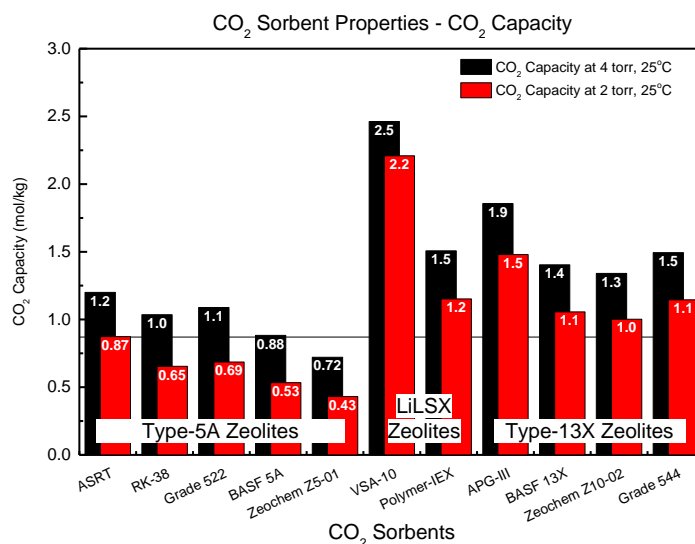


Figure 9. Equilibrium CO₂ capacity as calculated from Toth isotherms fit to measured pure component CO₂ isotherms within a pressure range of 0-20kPa at 25°C. CO₂ capacity of ASRT at 2 torr is denoted by a horizontal line for comparison.

The beds packed with ASRT were projected to operate for 3 years before maintenance based on flight data. RK-38 has already been used on the international space station and shown dusting rates which led to frequent system maintenance, an undesirable situation for CDRA and for a 4BMS supporting long-duration missions. The two binder-free materials, BASF 5A BF and BASF 13X BF, show high dusting rates and cannot be considered further. The crush strength of polymer-bound IEX is irrelevant due to eventual immobilization of this material into a packed bed monolith. Since crushing of pellets in the packed bed has not been found to be a sole root cause of dust production and since only three of the materials are equivalent to ASRT in pellet strength, crush strength alone can only eliminate

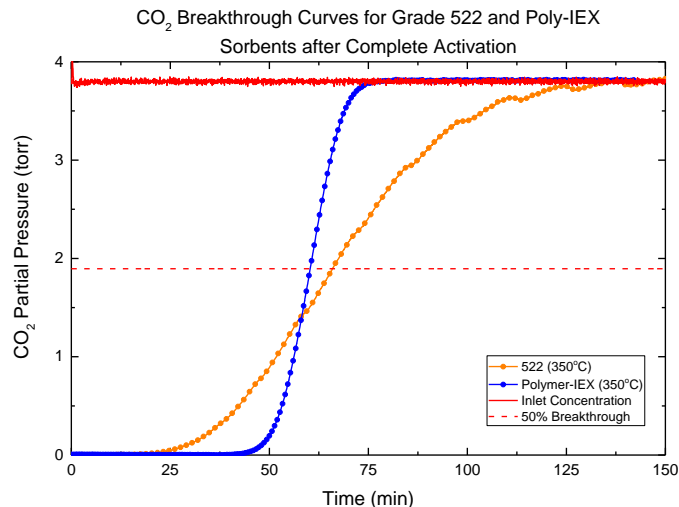


Figure 10. Breakthrough curve for Grade 522 5A and Polymer-IEX sorbent beds after activation at 350°C. The two beds are of nearly identical volume and aspect ratio. Breakthrough curves measured with an inlet feed of 3.8 torr CO₂ in dry N₂ at 10°C.

the number of thermal cycles has been shown to correlate with sorbent degradation in dry and humidified conditions.⁵ This is an exceptional case, but exemplifies the sometimes non-intuitive effects on productivity and efficiency in an integrated system. The results of dry CO₂ breakthrough indicate that the sorbents with the highest loading of CO₂ per bed volume will perform the best, thus the clay-bound LiLSX, VSA-10, appears to be the best selection under ideal conditions.

C. CO₂ sorption after recovery from moisture

Further studies with the HST focused on recovery of CO₂ capacity after exposure of the entire bed to water and subsequent regeneration at 204°C, the maximum attainable temperature in the system onboard the ISS. Figure 11 shows the extreme reduction in breakthrough performance of the LiLSX-based sorbents, VSA-10 and polymer-IEX, as well as the 13X sorbent APGIII after moisture exposure and activation at 204°C. These plots are overlaid with a type-5A material, Grade 522, to emphasize the reduction in bulk separation performance. This procedure was repeated on these four materials with the sequential test results shown in Figure 12.

The primary observation among these reactivated zeolites is the seemingly immutable CO₂ removal capacity of the type-5A zeolite. This removal capacity can be considered a baseline performance requirement for material selection during nominal and after recovery from off-nominal operation. In direct contrast to this result with the 5A zeolite is the

a bed packed with the polymer-bound material does not have as much active sorbent mass in the same volume. Another screening tool which has been adapted to study CO₂ breakthrough in packed beds is the Hydrothermal Stability Test (HST) stand.⁵ This instrument is able to run several small-scale packed beds sequentially with a choice of dry or humidified N₂ and CO₂ at cabin conditions. Figure 10 shows a comparison of the breakthrough curves of a 5A zeolite bed and of the polymer-bound zeolite bed.

One of the general results of this test is that the 5A and the polymer-bound LiLSX materials remove an equal amount of CO₂ in this configuration, but a system with the 5A material requires less overall power because of the longer time before 50% breakthrough (bulk separation) is achieved. The polymer-bound material has a significantly more ideal curve and would produce a more pure air product, but has a shorter breakthrough time. More rapid cycling leads to increased 4BMS system power requirements and

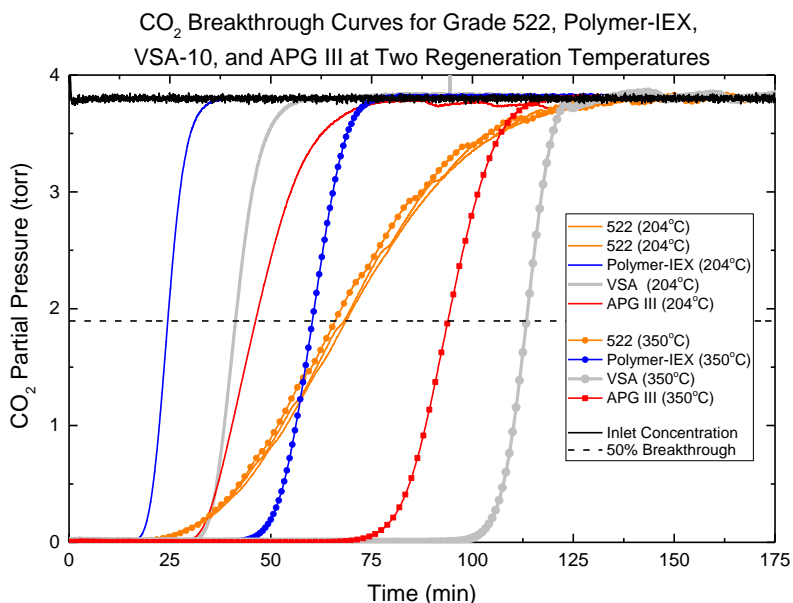


Figure 11. CO₂ breakthrough curves of Grade 522 5A, Polymer-IEX LiLSX, VSA-10 LiLSX, and APG III 13X sorbents after initial activation at 350°C and then after exposure to moisture and subsequent reactivation at 204°C. Breakthrough curves measured with an inlet feed of 3.8 torr CO₂ in dry N₂ at 10°C.

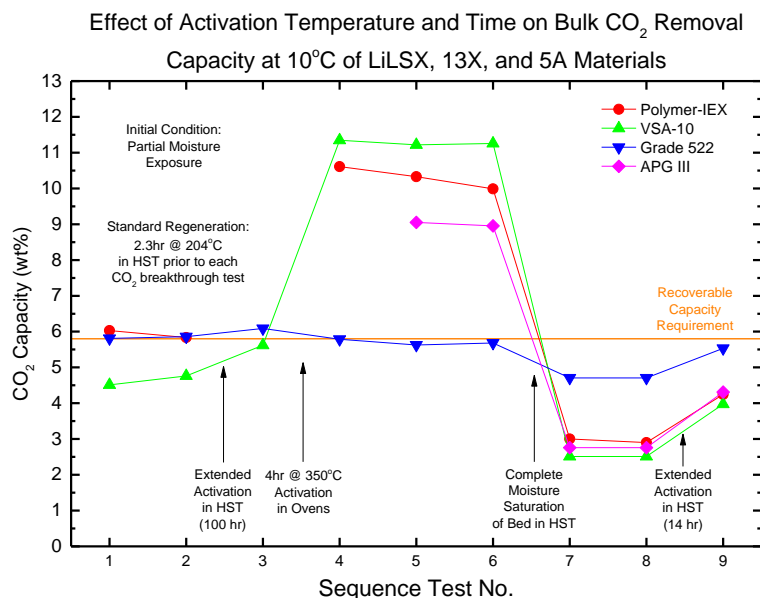


Figure 12. Bulk CO₂ removal capacity for VSA-10 LiLSX, Grade 522 5A, APGIII 13X, and Polymer-IEX LiLSX at 3.8 torr CO₂ and 10°C over the course of several tests after different activation procedures. Standard activation is a simulation of CDRA cycles, which is 204°C for 144 minutes in dry N₂. The activation temperature for each breakthrough test is listed on the x-axis and the resulting bulk CO₂ removal performance observed is shown on the y-axis. Results are reported on a per-bed-mass basis.

scenario where the entire sorbent bed was exposed to water vapor. Sequentially activating a single, conditioned sample at incrementally higher temperatures then probing the sample with CO₂ at 25°C after each cycle provides information on the extent of CO₂ capacity recovery. CO₂ adsorption is extremely sensitive to co-adsorbed water, therefore the extent of water removal is indirectly observed with this series of tests. Quantification of the amounts of co-adsorbed water will be reserved for future testing.

The results indicate that each class of zeolite retains significant amounts of water up to some characteristic temperature. It appears that most CO₂ capacity is recovered for the type-5A zeolite at temperatures below 150°C, for the type-13X zeolites at 225°C, and for the LiLSX zeolite at 275°C. Complete recovery of CO₂ capacity occurs at roughly 50°C higher than this temperature for a 4 hour activation cycle. Complete activation and full recovery of CO₂ removal capacity can also be achieved via extended time, as evidenced by the uptake after a 10 hour bakeout.

An immediate disagreement in the trend measured with the HST is found in the results here. The TGA results indicate that the 13X and LiLSX zeolites

sensitivity and incomplete recovery of CO₂ removal capability of the LiLSX-based zeolites. The results show that standard regeneration time and temperature of CDRA is insufficient to recover the CO₂ capacity of LiLSX and 13X zeolites, even to the level of the 5A zeolite. This translates to a risk of effectively permanent loss of CO₂ removal productivity, should moisture enter the bed. This high risk severely limits the opportunities to prepare a uniform bed of LiLSX and 13X materials for CDRA but options remain where layers of 5A zeolite are used to protect the selected sorbent. Future 4BMS designs may allow further use of these enabling CO₂ sorbents with minor system design changes such as higher attainable temperatures, bed recovery procedures, or bed layering.

Additional studies were conducted to characterize the recovery of CO₂ removal productivity in the event of moisture exposure. These tests were designed to assess the CO₂ working capacity of each sample after an attempt to recover from a worst-case

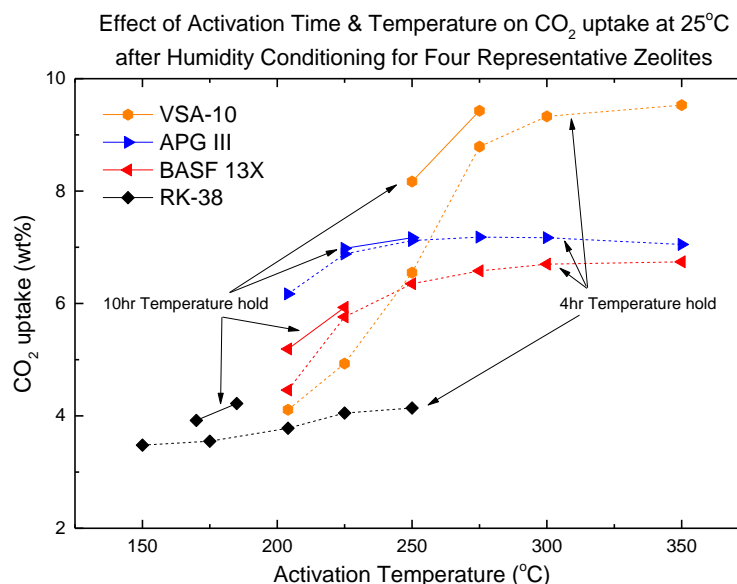


Figure 13. Humidity conditioned samples of 4 representative zeolites (type-5A, two type-13X, and LiLSX) tested for CO₂ uptake at 25°C and a composition of 0.5% CO₂ in N₂ after specific activation conditions. Samples were conditioned prior to a sequence of increasing activation temperatures where CO₂ uptake was probed between each cycle.

will adsorb more CO₂ than 5A zeolite after activation at 204°C. Several instrument differences prevent duplication of the test conditions at this time, therefore the HST results can be considered more accurate as the conditions are more representative of conditions in CDRA. The TGA test involves an adsorption temperature of 25°C, a smaller sample quantity in a suspended mesh pan configuration, and a continuous N₂ purge. The HST tests utilize a packed bed, adsorption at 10°C, and co-current desorption. These differences translate to significantly faster adsorption and desorption of the sample in the TGA. This timescale difference may be the reason for the disagreement between the trends observed with the HST versus the TGA and will be the target of future testing.

With the current results, it would appear that type-5A zeolites remain the lowest risk option with sufficient CO₂ removal capability. Additional results indicate that the high-performance 13X and LiLSX materials may not be high-risk materials and thus can still be considered. In order to minimize risk and maximize the lifetime of a 4BMS system, strong materials with low attrition in dry and humidified conditions will need to be selected. Collection of this information is ongoing in the structural studies detailed in the work submitted for publication by Watson.² Finally, for future 4BMS designs or minor CDRA modifications, a more in-depth study of the temperature and time required to recover sorbents from moisture exposure will be conducted.

IV. Conclusions and Future Work

For the guard layer and among the bulk desiccants, the results indicate that no changes need to be made for CDRA and for future 4BMS systems as the combination of properties found with the current materials is equal to or better than the tested alternatives. Among the residual desiccants, the present 13X zeolite remains the selection. Large-scale study of trace water vapor adsorption as well as its effects on structural properties would need to be conducted to provide sufficient reason to select a different residual desiccant.

Among the current set of CO₂ sorbents, no standout candidate can be readily selected though some have been eliminated. Material selection remains tightly integrated with the design of the system, with the latter limiting the number of sorbent choices. For CDRA, where only minimal changes can be made, the CO₂ sorbent selection is limited by the need to perform as well as the current 5A zeolite after regeneration from a water exposure event at the attainable temperature of 204°C. Additional results indicate that a 13X or LiLSX can be considered for the CO₂ removal bed in CDRA, as the worst case scenario would reduce their capacity to roughly equal to a 5A material. As the sorbent bed is large, one possibility is a layer of 5A zeolite protecting a layer of more water-sensitive zeolite with higher CO₂ capacity. Another possibility is a maintenance operation which regenerates the bed for an extended time to recover the CO₂ capacity of a 13X or LiLSX zeolite.

For a new 4BMS system, smaller CO₂ sorbent beds can be designed if a 13X or LiLSX zeolite is used due to the improved capacity and faster adsorption kinetics. The new bed would need to be designed to recover from exposure to water, an off-nominal event which has been observed in flight operations. This design must account for that risk and include the ability to recover to some acceptable performance level. Techniques include higher temperature bakeouts or extended, moderate temperature bakeouts. The results obtained in this work help to guide this risk assessment and thus future 4BMS designs.

Future work includes completing of the current data sets of structural properties and multi-temperature adsorption isotherms. Additionally, further evaluation of candidate samples for moisture recovery behavior in CDRA-like operation is needed to make a more fully informed selection for CDRA. Extending this study to potential 4BMS system designs would enable selection of the best sorbent for various design envelopes. Both of these studies will include cyclic testing with a range of activation time and temperature, vacuum, and adsorption at sub-ambient temperatures to better simulate conditions found in flight. Such a study would define requirements of a redesigned 4BMS for a candidate sorbent with the ability to recover from off-nominal events.

References

¹NASA. "Human Exploration & Operations (HEO)." 2016.

²Watson, D., Knox, J. C., West, P., and Bush, R. "Sorbent Structural Testing of Carbon Dioxide Removal Sorbents for Advanced Exploration Systems," *46th International Conference on Environmental Systems*. Vienna, 2016.

³Knox, J. C., Gostowski, R., Watson, D., Hogan, J. A., King, E., and Thomas, J. "Development of Carbon Dioxide Removal Systems for Advanced Exploration Systems," *International Conference on Environmental Systems*. AIAA, San Diego, 2012.

⁴Watson, D., Knox, J. C., West, P., Stanley, C., and Bush, R. "Sorbent Structural Impacts due to Humidity on Carbon Dioxide Removal Sorbents for Advanced Exploration Systems," *45th International Conference on Environmental Systems*. Bellevue, Washington, 2015.

⁵Knox, J. C., Gauto, H., and Miller, L. A. "Development of a Test for Evaluation of the Hydrothermal Stability of Sorbents used in Closed-Loop CO₂ Removal Systems," *International Conference on Environmental Systems*. Bellevue, Washington, 2015.

⁶Wang, Y., and LeVan, M. D. "Adsorption Equilibrium of Carbon Dioxide and Water Vapor on Zeolites 5A and 13X and Silica Gel: Pure Components," *Journal of Chemical and Engineering Data* Vol. 54, No. 10, 2009, pp. 2839-2844.

⁷Satish, U., Mendell, M. J., Shekhar, K., Hotchi, T., Sullivan, D., Streufert, S., and Fisk, W. J. "Is CO₂ an indoor pollutant? Direct effects of low-to-moderate CO₂ concentrations on human decision-making performance," *Environ Health Perspect* Vol. 120, No. 12, 2012, pp. 1671-7.

⁸Allen, J. G., MacNaughton, P., Satish, U., Santanam, S., Vallarino, J., and Spengler, J. D. "Associations of Cognitive Function Scores with Carbon Dioxide, Ventilation, and Volatile Organic Compound Exposures in Office Workers: A Controlled Exposure Study of Green and Conventional Office Environments," *Environ Health Perspect*, 2015.